Stabilized shock hydrodynamics: II. Design and physical interpretation of the SUPG operator for Lagrangian computations.

Guglielmo Scovazzi

Sandia National Laboratories

Stabilized shock hydrodynamics: II. Design and physical interpretation of the SUPG operator for Lagrangian computations.

Guglielmo Scovazzi
1431 Computational Shock- and Multi-physics Department
Sandia National Laboratories
P.O. Box 5800, MS 1110
Albuquerque, NM 87185-1110, USA
gscovaz@sandia.gov

Abstract

A new SUPG-stabilized formulation for Lagrangian Hydrodynamics of materials satisfying the Mie-Grüneisen equation of state was presented in the first paper of the series [7]. This article investigates in more detail the design of SUPG stabilization, focusing on its multiscale and physical interpretations. Connections with Kuropatenko's [5] analysis of shock-capturing operators in the limit of weak shocks are shown. Galilean invariance requirements for the SUPG operator are explored and corroborated by numerical evidence. This work is intended to elucidate the profound physical significance of the SUPG operator as a subgrid interaction model.

Acknowledgments

Contents

Appendix

List of Figures

Chapter 1

Introduction

The variational multiscale analysis proposed by Hughes and coauthors in [3, 4] is applied to the equations of Lagrangian hydrodynamics. The exact solution of the equations is decomposed into a *mesh-scale* component, resolvable by the numerical discretization (namely, a finite element method), and the *subgrid-scale* component, the complement to the exact solution of the mesh-scale component. The interaction between the subgrid-scale and the mesh-scale components of the solution can be represented by (approximately) solving a subgrid-scale problem, involving the element Green's function for the subgrid scales as the kernel of an inverse integral operator.

When applied in smooth regions of Lagrangian hydrodynamic flows, the multiscale analysis shows that the subgrid Green's function is an acoustical wave propagation kernel. Such result is proved for ideal gases and can be easily generalized to the case of Mie-Grüneisen materials. The purpose of the SUPG operator is to provide an efficient and effective representation of the interaction between the subgrid-scale and the mesh-scale solutions, ultimately resulting in the control of acoustical instabilities.

The importance of the Galilean invariance properties of the subgrid-scale solution is stressed. Although not present among the standard requirements for SUPG operators, the Galilean invariance principle appears to play a crucial role in obtaining reliable simulations of Lagrangian (highly transient) hydrodynamic flows. Numerical evidence is presented to support such findings.

Finally, a detailed analysis (in one dimension for ideal gases) highlights striking similarities between the SUPG operator and the correction of the original Von Neumann-Ricthmyer [12] viscosity proposed by Kuropatenko [5], in the limit for weak shocks. Some differences are present, since the Kuropatenko correction is applied only in compression regions of the flow domain, and the SUPG stabilization is applied on the whole computational domain, modulated by the local magnitude of the residual. Furthermore, the residual-based SUPG method prevents the overall accuracy to degrade to first order, contrary to the Kuropatenko approach, which relies solely on a modification of the artificial viscosity term.

The rest of the exposition is organized as follows: The variational multiscale analysis is developed in chapter 2, a discussion on Galilean invariance and subgrid-scale modeling is presented in chapter 3. Connections with the Kuropatenko artificial viscosity operator are presented in chapter 4, and conclusions are summarized in chapter 5.

Chapter 2

Variational multiscale analysis for Lagrangian hydrodynamics

In order to further analyze the Lagrangian SUPG approach developed in [7] a number of definitions are needed. The *deformation* $\boldsymbol{\varphi}$ is the transformation from the material to the Eulerian reference frame

$$
\begin{aligned}
\boldsymbol{\varphi} : V & \rightarrow & \Omega = \boldsymbol{\varphi}(V), & \qquad (2.1) \\
\boldsymbol{X} & \mapsto & \boldsymbol{x} = \boldsymbol{\varphi}(\boldsymbol{X}, t), & \quad \forall \boldsymbol{X} \in V, \ t \geq 0, \qquad (2.2)
\end{aligned}
$$

Here $\boldsymbol{X}$ is the material coordinate (which usually corresponds to the point vector in the initial configuration of the body), and $\boldsymbol{x}$ is the point vector in the Eulerian frame. V is the domain occupied by the body in the material reference frame. $\boldsymbol{\varphi}$ maps V to $\Omega(t)$, the domain occupied by the body in its current configuration (i.e., the domain occupied by the body at time t in the Eulerian reference frame). It will be assumed that $\boldsymbol{x}(\boldsymbol{X}, t{=}0) = \boldsymbol{X}$, implying $\Omega(t = 0) = V$. It is also useful to define the *deformation gradient* and its *Jacobian determinant*:

$$
\begin{aligned}
\boldsymbol{F} &= \nabla_{\boldsymbol{x}} \, \boldsymbol{\varphi} = \frac{\partial \varphi_i}{\partial X_j} = \frac{\partial x_i}{\partial X_j} & (2.3) \\
J &= \det \boldsymbol{F} & (2.4)
\end{aligned}
$$

Let us summarize the variational formulation for the Lagrangian hydrodynamics equations introduced in [7]. Given a partition $0 < t_1 < t_2 < \ldots < t_N = T$ of the time interval $I =]0, T[$, let $I_n =]t_n, t_{n+1}[$, so that $]0, T[= \bigcup_{n=0}^{N-1} I_n$. The space-time domain $Q = V \times I$ can be divided into time slabs

$$
Q_n = V \times I_n \qquad (2.5)
$$

with boundary $P_n = S \times I_n$ ($S = \partial V$ is the spatial boundary of V). The material domain V is further divided into material-subdomains V^e (elements in space, a partition of the initial configuration fixed with respect to time). Thus $V = \bigcup_{e=1}^{n_{el}} V^e$. A typical space-time element is given by $Q_n^e = V^e \times I_n$. The space-time boundary is also partitioned as $P_n = P_n^g \cup P_n^h$, $P_n^g \cap P_n^h = \emptyset$ (i.e., P_n is divided into a Dirichlet boundary P_n^g and a Neumann boundary P_n^h). Using the notation $\boldsymbol{V}(\boldsymbol{X}, t_n^{\pm}) = \lim_{t \to t_n^{\pm}} \boldsymbol{V}(\boldsymbol{X}, t)$, the classical space-time variational formulation reads:

Find $\boldsymbol{Y} \in \mathcal{S}^h$, such that $\forall \boldsymbol{W} \in \mathcal{V}^h$

$$\mathcal{B}(\boldsymbol{W}, \boldsymbol{Y}) = \mathcal{F}(\boldsymbol{W}) \tag{2.6}$$

$$
\begin{aligned}
\mathcal{B}(\boldsymbol{W}, \boldsymbol{Y}) = \ & \int_V \boldsymbol{W}(\boldsymbol{X}, t_{n+1}^-) \cdot \boldsymbol{U}(\boldsymbol{Y}(\boldsymbol{X}, t_{n+1}^-)) dV \\
& - \int_V \boldsymbol{W}(\boldsymbol{X}, t_n^+) \cdot \boldsymbol{U}(\boldsymbol{Y}(\boldsymbol{X}, t_n^-)) dV \\
& + \int_{Q_n} \left(-\boldsymbol{W}_{,t} \cdot \boldsymbol{U}(\boldsymbol{Y}) - \boldsymbol{W}_{,i} \cdot \boldsymbol{G}_i(\boldsymbol{Y}) + \boldsymbol{W} \cdot \boldsymbol{Z}(\boldsymbol{Y}) \right) \ dQ \\
& + \int_{P_n^g} \boldsymbol{W} \cdot \boldsymbol{G}_i(\boldsymbol{Y}) N_i \ dP
\end{aligned}
\tag{2.7}
$$

$$\mathcal{F}(\boldsymbol{W}) = -\int_{P_n^h} \boldsymbol{W} \cdot \boldsymbol{H}_i N_i \ dP - \int_{Q_n} \boldsymbol{W} \cdot \boldsymbol{B} \ dQ \tag{2.8}$$

where $\boldsymbol{H}_i$ represent the Neumann flux (a *traction*-type boundary condition in Lagrangian hydrodynamics), and, in the three-dimensional case,

$$
\boldsymbol{U} = \begin{bmatrix} u_1 \\ u_2 \\ u_3 \\ \rho_0 v_1 \\ \rho_0 v_2 \\ \rho_0 v_3 \\ \rho_0(e + \frac{1}{2} v_j v_j) \end{bmatrix}, \quad
\boldsymbol{Y} = \begin{bmatrix} u_1 \\ u_2 \\ u_3 \\ v_1 \\ v_2 \\ v_3 \\ p \end{bmatrix}, \quad
\boldsymbol{G}_i = \begin{bmatrix} 0 \\ 0 \\ 0 \\ p \operatorname{cof} F_{1i} \\ p \operatorname{cof} F_{2i} \\ p \operatorname{cof} F_{3i} \\ p v_j \operatorname{cof} F_{ji} \end{bmatrix}
\tag{2.9}
$$

$$
\boldsymbol{Z} = \begin{bmatrix} -v_1 \\ -v_2 \\ -v_3 \\ 0 \\ 0 \\ 0 \\ -\rho_0 g_j v_j \end{bmatrix}, \quad
\boldsymbol{B} = \begin{bmatrix} 0 \\ 0 \\ 0 \\ -\rho_0 g_1 \\ -\rho_0 g_2 \\ -\rho_0 g_3 \\ -\rho_0 s \end{bmatrix}
\tag{2.10}
$$
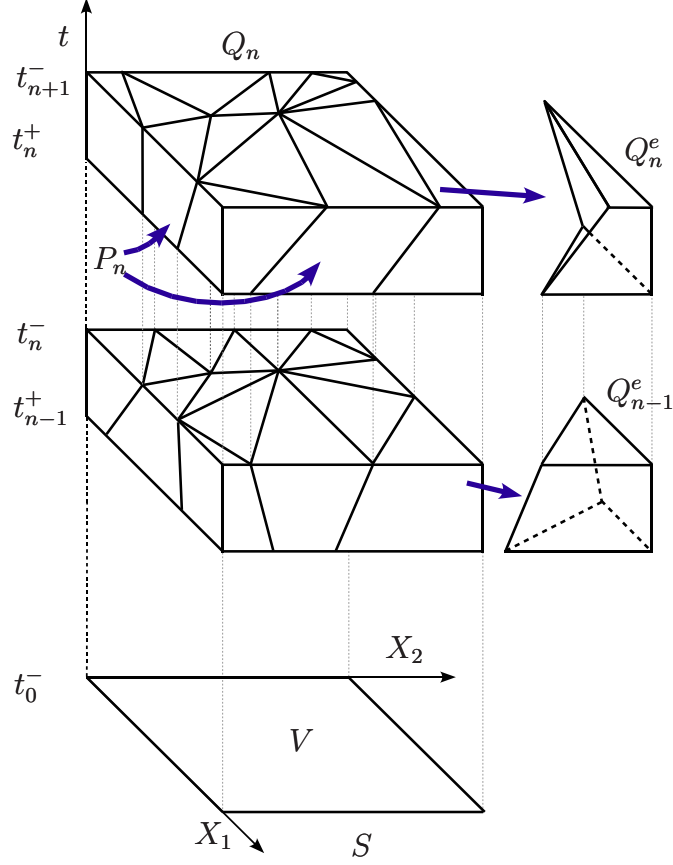
Figure 2.1. General finite element discretization in space-time.

Here, $\boldsymbol{u} = \boldsymbol{x} - \boldsymbol{X}$ is the displacement vector, $\boldsymbol{v}$ is the velocity vector, p is the pressure, ρ_0 is the initial (reference) density, e is the internal energy per unit mass, $\mathbf{cof}\,\boldsymbol{F} = J\boldsymbol{F}^{-T}$, $\boldsymbol{g}$ is a body force per unit mass, and s is a source/sink of energy per unit mass. The definitions of $\boldsymbol{U}$, $\boldsymbol{Y}$, $\boldsymbol{G}_i$, $\boldsymbol{Z}$, and $\boldsymbol{B}$ are consistent with [7], in which one- and two-dimensional computations were performed. For the moment, *complete* knowledge of the solution $\boldsymbol{Y}$ is assumed, so that neither SUPG stabilization nor discontinuity capturing operators are needed in the equations. For the sake of simplicity, it is assumed that the boundary conditions are of Dirichlet type, although the following derivations can be extended to boundary conditions of any type.

The multiscale analysis applies in regions of smooth flow. The solution $\boldsymbol{Y}$ can be decomposed into a *coarse-scale* (or *mesh-scale*) component $\boldsymbol{Y}^h \in \mathcal{S}^h$ (the component of $\boldsymbol{Y}$ resolved by the numerical mesh), and a *fine-scale* (or *subgrid-scale*) component $\boldsymbol{Y}' \in \mathcal{S}'$, ($\mathcal{S}' = \mathcal{S}/\mathcal{S}^h$ is the complement of $\mathcal{S}^h$ to $\mathcal{S}$). In particular, $\boldsymbol{Y}$ and $\boldsymbol{Y}^h$ are assumed *at least* continuous in space and time, and $\boldsymbol{Y}$ must be sufficiently smooth to

have

$$\boldsymbol{Y} = \boldsymbol{Y}^h + \boldsymbol{Y}' = \boldsymbol{Y}^h + \varepsilon\hat{\boldsymbol{Y}}', \text{with } \hat{\boldsymbol{Y}}' = O(\boldsymbol{Y}), \ \varepsilon << 1 \qquad (2.11)$$

In other words, $\boldsymbol{Y}'$ is small compared to $\boldsymbol{Y}$ and $\boldsymbol{Y}^h$.

Remark 1 *The assumptions of smoothness of $\boldsymbol{Y}$ and smallness of $\boldsymbol{Y}'$ hold, for example, in regions of isentropic flow. On the contrary, regularity and smallness of $\boldsymbol{Y}'$ are not verified near discontinuities, where the SUPG operator is not sufficient to stabilize the numerical computations. In other words, the dominant nonlinear dynamics in strong shocks is not appropriately captured by the multiscale approach, which hinges upon a local, linearized analysis.*

Remark 2 *The algorithm presented in [7] satisfies this continuity requirement for $\boldsymbol{Y}^h$. By definition, $\boldsymbol{Y}'$, is also continuous in regions where the flow is smooth. This aspect will lead to important simplifications in the subgrid-scale problem.*

With the previous key assumptions,

$$\boldsymbol{U}(\boldsymbol{Y}) \ = \ \boldsymbol{U}(\boldsymbol{Y}^h) + \varepsilon\boldsymbol{A}_0(\boldsymbol{Y}^h)\hat{\boldsymbol{Y}}' + O(\varepsilon^2) \approx \boldsymbol{U}(\boldsymbol{Y}^h) + \boldsymbol{A}_0(\boldsymbol{Y}^h)\boldsymbol{Y}' \qquad (2.12)$$

$$\boldsymbol{G}_i(\boldsymbol{Y}) \ = \ \boldsymbol{G}_i(\boldsymbol{Y}^h) + \varepsilon\boldsymbol{A}_i(\boldsymbol{Y}^h)\hat{\boldsymbol{Y}}' + O(\varepsilon^2) \approx \boldsymbol{G}_i(\boldsymbol{Y}^h) + \boldsymbol{A}_i(\boldsymbol{Y}^h)\boldsymbol{Y}' \qquad (2.13)$$

$$\boldsymbol{Z}(\boldsymbol{Y}) \ = \ \boldsymbol{Z}(\boldsymbol{Y}^h) + \varepsilon\boldsymbol{C}(\boldsymbol{Y}^h)\hat{\boldsymbol{Y}}' + O(\varepsilon^2) \approx \boldsymbol{Z}(\boldsymbol{Y}^h) + \boldsymbol{C}(\boldsymbol{Y}^h)\boldsymbol{Y}' \qquad (2.14)$$

For the moment, $\boldsymbol{A}_0$, $\boldsymbol{A}_i$, and $\boldsymbol{C}$ are given by the expressions:

$$\boldsymbol{A}_0(\boldsymbol{Y}^h) = \left.\frac{\partial \boldsymbol{U}}{\partial \boldsymbol{Y}}\right|_{\boldsymbol{Y}^h}, \quad \boldsymbol{A}_i(\boldsymbol{Y}^h) = \left.\frac{\partial \boldsymbol{G}_i}{\partial \boldsymbol{Y}}\right|_{\boldsymbol{Y}^h}, \quad \boldsymbol{C}(\boldsymbol{Y}^h) = \left.\frac{\partial \boldsymbol{Z}}{\partial \boldsymbol{Y}}\right|_{\boldsymbol{Y}^h} \qquad (2.15)$$

Remark 3 *To be precise, a slightly modified version of the previous definitions of $\boldsymbol{A}_0$, $\boldsymbol{A}_i$, and $\boldsymbol{C}$ is used in [7]. Namely, for the three-dimensional case, recalling $e = e(p, \rho_0, J)$,*

$$\boldsymbol{A}_0 = \left[\begin{array}{c|cccc} \boldsymbol{I}_{3\times 3} & \boldsymbol{0}_{3\times 1} & \boldsymbol{0}_{3\times 1} & \boldsymbol{0}_{3\times 1} & \boldsymbol{0}_{3\times 1} \\ \hline \boldsymbol{0}_{1\times 3} & \rho_0 & 0 & 0 & 0 \\ \boldsymbol{0}_{1\times 3} & 0 & \rho_0 & 0 & 0 \\ \boldsymbol{0}_{1\times 3} & 0 & 0 & \rho_0 & 0 \\ \boldsymbol{0}_{1\times 3} & 0 & 0 & 0 & \rho_0 e_{,p} \end{array}\right], \quad \boldsymbol{C} = \left[\begin{array}{c|cc} \boldsymbol{0}_{3\times 3} & -\boldsymbol{I}_{3\times 3} & \boldsymbol{0}_{3\times 1} \\ \hline \boldsymbol{0}_{4\times 3} & \boldsymbol{0}_{4\times 3} & \boldsymbol{0}_{4\times 1} \end{array}\right] \quad (2.16)$$

and

$$\boldsymbol{A}_i = \left[\begin{array}{c|cccc} \boldsymbol{0}_{3\times 3} & \boldsymbol{0}_{3\times 1} & \boldsymbol{0}_{3\times 1} & \boldsymbol{0}_{3\times 1} & \boldsymbol{0}_{3\times 1} \\ \hline \boldsymbol{0}_{1\times 3} & 0 & 0 & 0 & \mathrm{cof}\,F_{1i} \\ \boldsymbol{0}_{1\times 3} & 0 & 0 & 0 & \mathrm{cof}\,F_{2i} \\ \boldsymbol{0}_{1\times 3} & 0 & 0 & 0 & \mathrm{cof}\,F_{3i} \\ \boldsymbol{0}_{1\times 3} & (p+\rho_0 Je_{,J})\mathrm{cof}\,F_{1i} & (p+\rho_0 Je_{,J})\mathrm{cof}\,F_{2i} & (p+\rho_0 Je_{,J})\mathrm{cof}\,F_{3i} & 0 \end{array}\right]$$

$$(2.17)$$

for $i = 1, 2, 3$. The definitions $e_{,J} = \left.\frac{\partial e}{\partial J}\right|_p$ and $e_{,p} = \left.\frac{\partial e}{\partial p}\right|_J$, have been used. Expressions (2.16)–(2.17) have been derived by removing the kinetic energy equation from the total energy equation before performing Fréchet differentiation. Therefore, if defined as in [7],

$$\boldsymbol{A}_0(\boldsymbol{Y}^h) \neq \left.\frac{\partial \boldsymbol{U}}{\partial \boldsymbol{Y}}\right|_{\boldsymbol{Y}^h}, \quad \boldsymbol{A}_i(\boldsymbol{Y}^h) \neq \left.\frac{\partial \boldsymbol{G}_i}{\partial \boldsymbol{Y}}\right|_{\boldsymbol{Y}^h}, \quad \boldsymbol{C}(\boldsymbol{Y}^h) \neq \left.\frac{\partial \boldsymbol{Z}}{\partial \boldsymbol{Y}}\right|_{\boldsymbol{Y}^h} \tag{2.18}$$

Thanks to this modification, the stabilization operator constructed using (2.16)–(2.17) generates a perturbation to the test function space which respects Galilean invariance, an aspect further investigated in chapter 3. Straightforward use of (2.15) causes the perturbation to the Bubnov-Galerkin test function to be observer-dependent, in flagrant violation of the invariance principle.

The test function $\boldsymbol{W}$ can also be decomposed as $\boldsymbol{W} = \boldsymbol{W}^h + \boldsymbol{W}'$, $\boldsymbol{W}' \in \mathcal{V}' = \mathcal{V}/\mathcal{V}^h$, and it is assumed that $\mathcal{V}'$ and $\mathcal{V}^h$, as well as $\mathcal{S}'$ and $\mathcal{S}^h$, are *linearly independent*.

2.1   Mesh-scale equation

The mesh-scale equation is obtained by testing (2.6) in $\mathcal{V}^h$:

$$
\begin{aligned}
0 =\ & \int_V \boldsymbol{W}^h(\boldsymbol{X}, t_{n+1}) \cdot \boldsymbol{U}(\boldsymbol{Y}^h(\boldsymbol{X}, t_{n+1})) dV - \int_V \boldsymbol{W}^h(\boldsymbol{X}, t_n) \cdot \boldsymbol{U}(\boldsymbol{Y}^h(\boldsymbol{X}, t_n)) dV \\
& \int_V \boldsymbol{W}^h(\boldsymbol{X}, t_{n+1}) \cdot \boldsymbol{A}_0 \boldsymbol{Y}'(\boldsymbol{X}, t_{n+1}) dV - \int_V \boldsymbol{W}^h(\boldsymbol{X}, t_n) \cdot \boldsymbol{A}_0 \boldsymbol{Y}'(\boldsymbol{X}, t_n) dV \\
& + \int_{Q_n} \left(-\boldsymbol{W}^h_{,t} \cdot \boldsymbol{U}(\boldsymbol{Y}^h) - \boldsymbol{W}^h_{,i} \cdot \boldsymbol{G}_i(\boldsymbol{Y}^h) + \boldsymbol{W}^h \cdot \boldsymbol{Z}(\boldsymbol{Y}^h) + \boldsymbol{W}^h \cdot \boldsymbol{B} \right)\ dQ \\
& + \int_{Q_n} \left(-\boldsymbol{W}^h_{,t} \cdot \boldsymbol{A}_0 \boldsymbol{Y}' - \boldsymbol{W}^h_{,i} \cdot \boldsymbol{A}_i \boldsymbol{Y}' + \boldsymbol{W}^h \cdot \boldsymbol{C} \boldsymbol{Y}' \right)\ dQ \\
& + \int_{P_n^g} \boldsymbol{W}^h \cdot \left(\boldsymbol{G}_i(\boldsymbol{Y}) + \boldsymbol{A}_i \boldsymbol{Y}' \right) N_i\ dP
\end{aligned}
\tag{2.19}
$$

or, more succinctly,

$$
\begin{aligned}
0 \;=\; & \mathcal{B}(\boldsymbol{W}^h, \boldsymbol{Y}^h) - \mathcal{F}(\boldsymbol{W}^h) + \int_{Q_n} \mathcal{L}_{SH}^* \boldsymbol{W}^h \cdot \boldsymbol{Y}' dQ \\
& + \int_{P_n^g} \boldsymbol{W}^h \cdot \boldsymbol{A}_i \boldsymbol{Y}' N_i \; dP \\
& + \int_V \boldsymbol{W}^h(\boldsymbol{X}, t_{n+1}) \cdot \boldsymbol{A}_0 \boldsymbol{Y}'(\boldsymbol{X}, t_{n+1}) dV \\
& - \int_V \boldsymbol{W}^h(\boldsymbol{X}, t_n) \cdot \boldsymbol{A}_0 \boldsymbol{Y}'(\boldsymbol{X}, t_n) dV
\end{aligned}
\tag{2.20}
$$

with $\mathcal{L}_{SH}^* = -\boldsymbol{A}_0^T \partial_t - \boldsymbol{A}_i^T \partial_i + \boldsymbol{C}^T$ ($\mathcal{L}_{SH} = \boldsymbol{A}_0 \partial_t + \boldsymbol{A}_i \partial_i + \boldsymbol{C}$). Typically, in the SUPG stabilization context, it is assumed that the space-time boundary integrals involving $\boldsymbol{Y}'$ vanish, namely

$$
\int_{P_n^g} \boldsymbol{W}^h \cdot \boldsymbol{A}_i \boldsymbol{Y}' N_i \; dP \;=\; 0
\tag{2.21}
$$

$$
\int_V \boldsymbol{W}^h(\boldsymbol{X}, t_{n+1}) \cdot \boldsymbol{A}_0 \boldsymbol{Y}'(\boldsymbol{X}, t_{n+1}) dV \;=\; 0
\tag{2.22}
$$

$$
\int_V \boldsymbol{W}^h(\boldsymbol{X}, t_n) \cdot \boldsymbol{A}_0 \boldsymbol{Y}'(\boldsymbol{X}, t_n) dV \;=\; 0
\tag{2.23}
$$

Remark 4 *Notice that there is no theoretical basis for such requirements, other than simplifications at the implementation level. The boundary integral in (2.21) can be justified to vanish by assuming that the solution is fully known at the boundary, where only Dirichlet conditions are prescribed. Assumptions (2.22)–(2.23), instead, have no specific rationale.*

Remark 5 *The previous remark can also be interpreted from a reverse perspective, since the decomposition of $\boldsymbol{Y}$ into $\boldsymbol{Y}^h$ and $\boldsymbol{Y}'$ has a certain degree of arbitrariness. In other words, one could assume (2.21)–(2.22) as part of the definition of $\boldsymbol{Y}'$, and, consequently, obtain $\boldsymbol{Y}^h$ as its complement to $\boldsymbol{Y}$.*

Using (2.21)–(2.23), (2.20) takes the simple form

$$
\boxed{\mathcal{B}(\boldsymbol{W}^h, \boldsymbol{Y}^h) + \int_{Q_n} \mathcal{L}_{SH}^* \boldsymbol{W}^h \cdot \boldsymbol{Y}' \; dQ = 0}
\tag{2.24}
$$

2.2 Subgrid-scale equation

The subgrid-scale equation is used in stabilized methods to provide an approximation to $\boldsymbol{Y}'$ in (2.24). If $\boldsymbol{Y}$ has enough regularity, integration by parts can be performed

without generating distributional integrals, and the Euler-Lagrange equations can be recovered from (2.6), namely

$$\int_{Q_n} \boldsymbol{W} \cdot (\boldsymbol{U}_{,t}(\boldsymbol{Y}) + \boldsymbol{G}_{i,i}(\boldsymbol{Y}) + \boldsymbol{Z}(\boldsymbol{Y}) + \boldsymbol{B}) \ dQ \quad = \quad 0 \tag{2.25}$$

where the jump term in time vanishes by continuity of the solution $\boldsymbol{Y}$. Substituting (2.12)–(2.14) into (2.25), tested on $\mathcal{V}'$, yields

$$\int_{Q_n} \boldsymbol{W}' \cdot (\mathcal{L}_{SH}\boldsymbol{Y}' + \boldsymbol{U}_{,t}(\boldsymbol{Y}^h) + \boldsymbol{G}_{i,i}(\boldsymbol{Y}^h) + \boldsymbol{Z}(\boldsymbol{Y}^h) + \boldsymbol{B}) \ dQ = 0 \tag{2.26}$$

It is possible to further manipulate (2.26) and obtain

$$\boxed{\int_{Q_n} \boldsymbol{W}' \cdot \mathcal{L}_{SH}\boldsymbol{Y}' \ dQ \approx - \int_{Q_n} \boldsymbol{W}' \cdot \boldsymbol{Res}(\boldsymbol{Y}^h) \ dQ} \tag{2.27}$$

where, $\boldsymbol{Res}(\boldsymbol{Y}^h) = \mathcal{L}_{SH}\boldsymbol{Y}^h + \boldsymbol{B}$.

Remark 6 *This last step, namely*

$$\boldsymbol{U}_{,t}(\boldsymbol{Y}^h) + \boldsymbol{G}_{i,i}(\boldsymbol{Y}^h) + \boldsymbol{Z}(\boldsymbol{Y}^h) \approx \mathcal{L}_{SH}\boldsymbol{Y}^h \tag{2.28}$$

holds as long as the assumption $\boldsymbol{Y}' << \boldsymbol{Y}^h, \boldsymbol{Y}$ holds. As the mesh is refined in smooth regions of the solution, $\boldsymbol{Y}' \to \boldsymbol{0}$, and the approximation expressed by (2.28) becomes increasingly more accurate. This is clearly not the case near discontinuities.

2.2.1 Subgrid-scale Green's function

Solving (2.27) for $\boldsymbol{Y}'$ yields a way to incorporate the effect of the subgrid solution into the *resolved* mesh scale equation (2.24). To solve (2.27), the inverse operator of $\mathcal{L}_{SH}$ in the subgrid space $\mathcal{V}'$ has to be computed. $\mathcal{L}_{SH}^{-1}$ is an integral operator with a matrix Green's function kernel. Namely,

$$\boldsymbol{Y}' \quad = \quad \mathcal{L}_{SH}^{-1}(-\boldsymbol{Res}(\boldsymbol{Y}^h)) = - \int_{Q_n} \boldsymbol{G}'_{SH} \ \boldsymbol{Res}(\boldsymbol{Y}^h) \ dQ, \text{ in } \mathcal{V}'(Q_n) \tag{2.29}$$

Remark 7 *Notice that, in general, the subgrid-scale problem is nonlocal.*

17

Remark 8 *A local approximation can be found as follows:*

$$\boldsymbol{Y}' \approx \sum_{e=1}^{n_{el}} \boldsymbol{Y}'_{Q_n^e} \chi_{Q_n^e} \tag{2.30}$$

where $\chi_{Q_n^e}$ is the characteristic function relative to the element domain Q_n^e, and

$$\boldsymbol{Y}'_{Q_n^e} = -\int_{Q_n^e} \boldsymbol{G}'_{SH} \, \boldsymbol{Res}(\boldsymbol{Y}^h) \, dQ, \ in \ \mathcal{V}'(Q_n^e) \tag{2.31}$$

Expressions (2.30)–(2.31) introduce an element localization of (2.29). Although such approach introduces an error, it drastically simplifies the subgrid problem, which decouples element-wise.

Following the approach in standard SUPG-stabilized methods, the local Green's function $\boldsymbol{G}'_{SH}$ in (2.31) is approximated as follows:

$$
\begin{aligned}
\boldsymbol{Y}'_{Q_n^e}(\boldsymbol{X}) &= -\int_{Q_n^e} \boldsymbol{G}'_{SH}(\boldsymbol{X}, \tilde{\boldsymbol{X}}; t, \tilde{t}) \, \boldsymbol{Res}(\boldsymbol{Y}^h(\tilde{\boldsymbol{X}}; \tilde{t})) \, dQ_{\{\tilde{X}, \tilde{t}\}} \\
&\approx -\int_{Q_n^e} \boldsymbol{\tau}(\boldsymbol{X}; t) \, \delta(\tilde{\boldsymbol{X}} - \boldsymbol{X}; t - \tilde{t}) \, \boldsymbol{Res}(\boldsymbol{Y}^h(\tilde{\boldsymbol{X}}, \tilde{t})) \, dQ_{\{\tilde{X}, \tilde{t}\}} \\
&= -\boldsymbol{\tau}(\boldsymbol{X}; t) \, \boldsymbol{Res}(\boldsymbol{Y}^h(\boldsymbol{X}; t))
\end{aligned}
\tag{2.32}
$$

where $\delta(\tilde{\boldsymbol{X}} - \boldsymbol{X}; t - \tilde{t})$ is the space-time Dirac distribution. The term $\boldsymbol{\tau}(\boldsymbol{X}; t)$ is in general obtained by means of a local splitting of the solution, and sometimes takes a simple diagonal form. For more details on the techniques used to design the SUPG operator, the reader can refer to [2, 7, 8, 10, 9, 11].

Remark 9 *Equation (2.32) represents a further localization of (2.31), since the Green's function kernel is approximated by a Dirac distribution.*

Given the proposed approximation to $\boldsymbol{Y}'$, it is possible to feed back the subgrid information into the mesh scale equation (2.24):

$$\boxed{\mathcal{B}(\boldsymbol{W}^h, \boldsymbol{Y}^h) - \sum_{e=1}^{(n_{el})_n} \int_{Q_n^e} \mathcal{L}^*_{SH} \boldsymbol{W}^h \cdot \boldsymbol{\tau} \, \boldsymbol{Res}(\boldsymbol{Y}^h) = 0} \tag{2.33}$$

Remark 10 *Equation (2.33) expresses the so-called variational multiscale stabilization term, which, in general, differs from the standard SUPG term because of the presence of the matrix $\boldsymbol{C}^T$ in $\mathcal{L}^*_{SH}$. However, in the present context, the SUPG and variational multiscale terms are identical, since, as mentioned in [7], the stabilization affects only the momentum and energy equations, to which $\boldsymbol{C}^T$ gives no contribution.*

2.2.2 Subgrid-scale Euler equations

It is instructive to derive the subgrid-scale Euler equations to gain familiarity with the structure of the subgrid problem. The momentum and energy equations in Lagrangian coordinates read

$$0 \;=\; \rho_0 \left.\frac{\partial v_i}{\partial t}\right|_{\boldsymbol{X}} + \frac{\partial}{\partial X_j}(p \, \mathrm{cof}\,F_{ij}) - \rho_0 g_i \tag{2.34}$$

$$0 \;=\; \rho_0 \left.\frac{\partial}{\partial t}\right|_{\boldsymbol{X}}\left(e + \frac{v_k v_k}{2}\right) + \frac{\partial}{\partial X_j}(v_i p \, \mathrm{cof}\,F_{ij}) - \rho_0 g_k v_k - \rho_0 s \tag{2.35}$$

Recalling the Piola identity, $\partial_{X_j}\mathrm{cof}\,F_{ij} = 0$, a more succinct form of the equations can be obtained, namely

$$0 \;=\; Res_i^v(\boldsymbol{Y}, \rho_0; p, \boldsymbol{v}) \tag{2.36}$$

$$\begin{aligned}0 \;&=\; Res^E(\boldsymbol{Y}, \rho_0; p, \boldsymbol{v}) \\ &=\; v_i \, Res_i^v(\boldsymbol{Y}, \rho_0; p, \boldsymbol{v}) + Res^e(\boldsymbol{Y}, \rho_0; p, \boldsymbol{v})\end{aligned} \tag{2.37}$$

where the definitions

$$Res_i^v(\boldsymbol{Y}, \rho_0; q, \boldsymbol{w}) \;=\; \mathcal{L}_{SH_i}^v(q, \boldsymbol{w}) - \rho_0 g_i \tag{2.38}$$

$$\mathcal{L}_{SH_i}^v(q, \boldsymbol{w}) \;=\; \rho_0 \left.\frac{\partial w_i}{\partial t}\right|_{\boldsymbol{X}} + \frac{\partial q}{\partial X_j}\,\mathrm{cof}\,F_{ij} \tag{2.39}$$

$$Res^e(\boldsymbol{Y}, \rho_0; q, \boldsymbol{w}) \;=\; \mathcal{L}_{SH}^e(q, \boldsymbol{w}) - \rho_0 s \tag{2.40}$$

$$\mathcal{L}_{SH}^e(q, \boldsymbol{w}) \;=\; \rho_0 e_{,p} \left.\frac{\partial q}{\partial t}\right|_{\boldsymbol{X}} + (p + \rho_0 J e_{,J})\frac{\partial w_i}{\partial X_j}\,\mathrm{cof}\,F_{ij} \tag{2.41}$$

have been used. Applying (2.27), and assuming, as in [7] piecewise linear continuous interpolation, it is easy to derive

$$\rho_0^h \left. \frac{\partial v_i'}{\partial t} \right|_{\boldsymbol{X}} + \frac{\partial p'}{\partial X_j} \text{cof} F_{ij}^h = -\rho_0^h \left. \frac{\partial v_i^h}{\partial t} \right|_{\boldsymbol{X}} - \frac{\partial p^h}{\partial X_j} \text{cof} F_{ij}^h$$
$$-\rho_0^h g_i + O(h^2) \tag{2.42}$$

$$\rho_0^h e_{,p}^h \left. \frac{\partial p'}{\partial t} \right|_{\boldsymbol{X}}$$
$$+\frac{\partial v_i'}{\partial X_j}(p^h + \rho_0^h J e_{,J}^h) \text{cof} F_{ij}^h$$
$$+v_k^h \left(\rho_0^h \left. \frac{\partial v_k'}{\partial t} \right|_{\boldsymbol{X}} + \frac{\partial p'}{\partial X_j} \text{cof} F_{kj}^h \right) = -v_k^h \left(\rho_0^h \left. \frac{\partial v_k^h}{\partial t} \right|_{\boldsymbol{X}} + \frac{\partial p^h}{\partial X_k} \text{cof} F_{ij}^h - \rho_0^h g_k \right)$$
$$-\rho_0^h e_{,p}^h \left. \frac{\partial p^h}{\partial t} \right|_{\boldsymbol{X}}$$
$$-\frac{\partial v_i^h}{\partial X_i}(p^h + \rho_0^h J e_{,J}^h) \text{cof} F_{ij}^h$$
$$-\rho_0^h s + O(h^2) \tag{2.43}$$

where (2.42)–(2.43) hold in a weak sense, tested on the space $\mathcal{V}'$. Using (2.38) and (2.40), equations (2.42)–(2.43) can be cast more compactly as

$$\mathcal{L}_{SH_i}^{\boldsymbol{v}}(p', \boldsymbol{v}') = -Res_i^{\boldsymbol{v}}(\boldsymbol{Y}^h; p^h, \boldsymbol{v}^h) + O(h^2), \quad \text{in } \mathcal{V}' \tag{2.44}$$

$$\mathcal{L}_{SH}^e(p', \boldsymbol{v}') + v_i^h \mathcal{L}_{SH_i}^{\boldsymbol{v}}(p', \boldsymbol{v}') = -v_i^h Res_i^{\boldsymbol{v}}(\boldsymbol{Y}^h; p^h, \boldsymbol{v}^h)$$
$$-Res_i^e(\boldsymbol{Y}^h; p^h, \boldsymbol{v}^h) + O(h^2), \quad \text{in } \mathcal{V}' \tag{2.45}$$

It is immediate to realize that equation (2.45) contains the product of equation (2.44) and v_i^h. This term can be simplified without perturbing the overall accuracy of the subgrid approximation, yielding a form of the residual less expensive to compute, namely

$$\mathcal{L}_{SH_i}^{\boldsymbol{v}}(p', \boldsymbol{v}') = -Res_i^{\boldsymbol{v}}(\boldsymbol{Y}^h; p^h, \boldsymbol{v}^h) + O(h^2), \text{ in } \mathcal{V}' \tag{2.46}$$

$$\mathcal{L}_{SH}^e(p', \boldsymbol{v}') = -Res_i^e(\boldsymbol{Y}^h; p^h, \boldsymbol{v}^h) + O(h^2), \text{ in } \mathcal{V}' \tag{2.47}$$

Remark 11 *From the algebraic point of view, the proposed simplification corresponds to a block Gaussian elimination strategy in the solution of the subgrid-scale problem.*

Remark 12 *The proposed approach is "minimalist", in the sense that only the key components of the residual are retained, namely, the advective form of the momentum*

20

and internal energy equations. It was shown in [7] that the stability properties of the overall formulation are unaffected by this procedure.

Remark 13 *Assuming that, in a weak sense in $\mathcal{V}'$,*

$$\mathcal{L}^{\boldsymbol{v}}_{SH_i}(p', \boldsymbol{v}') \;=\; Res^{\boldsymbol{v}}_i(\boldsymbol{Y}^h; p^h, \boldsymbol{v}^h) + O(h^2) \tag{2.48}$$

implies

$$v_i^h \mathcal{L}^{\boldsymbol{v}}_{SH_i}(p', \boldsymbol{v}') \;=\; -v_i^h Res^{\boldsymbol{v}}_i(\boldsymbol{Y}^h; p^h, \boldsymbol{v}^h) + O(h^2) \tag{2.49}$$

is reasonable if $\boldsymbol{v}^h$ varies smoothly and its values are not excessively high. For the simulations presented in [7] this assumption seemed appropriate.

2.2.3   An example: Linearized gas dynamics equations

Let us further analyze the subgrid-scale equations. For an ideal gas, $p = (\gamma - 1)\rho_0 e / J$, so that

$$\rho_0 e_{,p} \;=\; \frac{J}{\gamma - 1} \tag{2.50}$$

$$p + \rho_0 J e_{,J} \;=\; \frac{\gamma}{\gamma - 1} p \tag{2.51}$$

For the sake of simplicity, we will consider the equations over a single element. It will be assumed that $\overline{\boldsymbol{Y}}$ is a globally discontinuous, element-wise constant approximation to $\boldsymbol{Y}^h$. We will also use the simplified form of the subgrid-scale problem as in (2.46)–(2.47). Hence,

$$\mathcal{L}_{SH}\boldsymbol{Y}' \approx -\boldsymbol{Res}(\boldsymbol{Y}^h), \text{ in } \mathcal{V}'(Q_n^e) \tag{2.52}$$

reduces to

$$\bar{\rho}_0 \left.\frac{\partial v_i'}{\partial t}\right|_{\boldsymbol{x}} + \frac{\partial p'}{\partial X_j}\mathrm{cof}\bar{F}_{ij} \;\approx\; -Res^{\boldsymbol{v}}_i(\overline{\boldsymbol{Y}}; \bar{\boldsymbol{v}}, \bar{p}) \tag{2.53}$$

$$\frac{\bar{J}}{\gamma - 1}\left.\frac{\partial p'}{\partial t}\right|_{\boldsymbol{x}} + \frac{\gamma}{\gamma - 1}\bar{p}\,\mathrm{cof}\bar{F}_{ij}\frac{\partial v_i'}{\partial X_j} \;\approx\; -Res^e(\overline{\boldsymbol{Y}}; \bar{\boldsymbol{v}}, \bar{p}) \tag{2.54}$$

Taking the time derivative $\partial_t|_{\boldsymbol{X}}$ of (2.53), and applying the gradient operator $\partial_{X_l}\mathrm{cof}\,\bar{F}_{kl}$ to (2.54),

$$\bar{\rho}_0\left.\frac{\partial^2 v_i'}{\partial t^2}\right|_{\boldsymbol{X}} + \left.\frac{\partial}{\partial t}\right|_{\boldsymbol{X}}\left(\frac{\partial p'}{\partial X_j}\right)\mathrm{cof}\,\bar{F}_{ij} \;\approx\; -\left.\frac{\partial}{\partial t}\right|_{\boldsymbol{X}}\left(Res_i^v(\overline{\boldsymbol{Y}};\bar{\boldsymbol{v}},\bar{p})\right) \tag{2.55}$$

$$\frac{\partial}{\partial X_l}\left(\left.\frac{\partial p'}{\partial t}\right|_{\boldsymbol{X}}\right)\mathrm{cof}\,\bar{F}_{kl}$$
$$+\frac{\gamma}{\bar{J}}\bar{p}\,\mathrm{cof}\,\bar{F}_{ij}\mathrm{cof}\,\bar{F}_{kl}\frac{\partial^2 v_i'}{\partial X_j \partial X_l} \;\approx\; -\frac{\gamma-1}{\bar{J}}\mathrm{cof}\,\bar{F}_{kl}\frac{\partial}{\partial X_l}\left(Res^e(\overline{\boldsymbol{Y}};\bar{\boldsymbol{v}},\bar{p})\right) \tag{2.56}$$

Subtracting (2.56) from (2.55) yields

$$\bar{\rho}_0\left.\frac{\partial^2 v_i'}{\partial t^2}\right|_{\boldsymbol{X}} - \frac{\gamma}{\bar{J}}\bar{p}\,\mathrm{cof}\,\bar{F}_{ij}\mathrm{cof}\,\bar{F}_{kl}\frac{\partial^2 v_k'}{\partial X_l \partial X_j} \;\approx\; \frac{\gamma-1}{\bar{J}}\mathrm{cof}\,\bar{F}_{ij}\frac{\partial}{\partial X_j}\left(Res^e(\overline{\boldsymbol{Y}};\bar{\boldsymbol{v}},\bar{p})\right)$$
$$-\left.\frac{\partial}{\partial t}\right|_{\boldsymbol{X}}\left(Res_i^v(\overline{\boldsymbol{Y}};\bar{\boldsymbol{v}},\bar{p})\right) \tag{2.57}$$

Viceversa, taking the time derivative $\partial_t|_{\boldsymbol{X}}$ of (2.54), and applying the divergence operator $\partial_{X_l}\mathrm{cof}\,\bar{F}_{il}$ to (2.53),

$$\frac{\partial}{\partial X_l}\left(\left.\frac{\partial v_i'}{\partial t}\right|_{\boldsymbol{X}}\right)\mathrm{cof}\,\bar{F}_{il}$$
$$+\frac{1}{\bar{\rho}_0}\frac{\partial^2 p'}{\partial X_j \partial X_l}\mathrm{cof}\,\bar{F}_{ij}\mathrm{cof}\,\bar{F}_{il} \;\approx\; -\frac{1}{\bar{\rho}_0}\frac{\partial}{\partial X_l}\left(Res_i^v(\overline{\boldsymbol{Y}};\bar{\boldsymbol{v}},\bar{p})\right)\mathrm{cof}\,\bar{F}_{il} \tag{2.58}$$

$$\left.\frac{\partial^2 p'}{\partial t^2}\right|_{\boldsymbol{X}} + \frac{\gamma}{\bar{J}}\bar{p}\left.\frac{\partial}{\partial t}\right|_{\boldsymbol{X}}\left(\frac{\partial v_i'}{\partial X_j}\right)\mathrm{cof}\,\bar{F}_{ij} \;\approx\; -\frac{\gamma-1}{\bar{J}}\left.\frac{\partial}{\partial t}\right|_{\boldsymbol{X}}\left(Res^e(\overline{\boldsymbol{Y}};\bar{\boldsymbol{v}},\bar{p})\right) \tag{2.59}$$

Subtracting (2.58) from (2.59) gives

$$\left.\frac{\partial^2 p'}{\partial t^2}\right|_{\boldsymbol{X}} - \frac{\gamma\,p}{\bar{J}\bar{\rho}_0}\frac{\partial^2 p'}{\partial X_j \partial X_l}\mathrm{cof}\,\bar{F}_{ij}\mathrm{cof}\,\bar{F}_{il} \;\approx\; \frac{\gamma\,p}{\bar{J}\bar{\rho}_0}\frac{\partial}{\partial X_l}\left(Res_i^v(\overline{\boldsymbol{Y}};\bar{\boldsymbol{v}},\bar{p})\right)\mathrm{cof}\,\bar{F}_{il}$$
$$-\frac{\gamma-1}{\bar{J}}\left.\frac{\partial}{\partial t}\right|_{\boldsymbol{X}}\left(Res^e(\overline{\boldsymbol{Y}};\bar{\boldsymbol{v}},\bar{p})\right) \tag{2.60}$$

It is possible to transform the previous equations in the current configuration (Eulerian reference frame), assuming $\mathbf{cof}\,\boldsymbol{F} \approx \mathbf{cof}\,\bar{\boldsymbol{F}}$, and recalling that

$$\frac{\partial f}{\partial X_j}\mathrm{cof}\,F_{ij} \;=\; J\frac{\partial f}{\partial x_i} \tag{2.61}$$

$$\frac{\partial^2 f}{\partial X_j \partial X_l}\mathrm{cof}\,F_{ij}\mathrm{cof}\,F_{kl} \;=\; J^2\frac{\partial^2 f}{\partial x_i \partial x_k} \tag{2.62}$$

22

Thus, (2.57) and (2.60) yield

$$
\left.\frac{\partial^2 v_i'}{\partial t^2}\right|_{\boldsymbol{X}} - \bar{c}_s^2 \frac{\partial^2 v_i'}{\partial x_j \partial x_j} \approx \frac{1}{\bar{\rho}_0}\left(-\left.\frac{\partial}{\partial t}\right|_{\boldsymbol{X}}\left(Res_i^{\boldsymbol{v}}(\overline{\boldsymbol{Y}};\bar{\boldsymbol{v}},\bar{p})\right)\right.
$$
$$
\left.(\gamma-1)\frac{\partial}{\partial x_i}\left(Res^e(\overline{\boldsymbol{Y}};\bar{\boldsymbol{v}},\bar{p})\right)\right) \tag{2.63}
$$

$$
\left.\frac{\partial^2 p'}{\partial t^2}\right|_{\boldsymbol{X}} - \bar{c}_s^2\,\frac{\partial^2 p'}{\partial x_i^2} \approx \frac{1}{\bar{J}}\left(\bar{c}_s^2 \frac{\partial}{\partial x_i}\left(Res_i^{\boldsymbol{v}}(\overline{\boldsymbol{Y}};\bar{\boldsymbol{v}},\bar{p})\right)\right.
$$
$$
\left.-(\gamma-1)\left.\frac{\partial}{\partial t}\right|_{\boldsymbol{X}}\left(Res^e(\overline{\boldsymbol{Y}};\bar{\boldsymbol{v}},\bar{p})\right)\right) \tag{2.64}
$$

or, in vector form,

$$
\left.\frac{\partial^2 \boldsymbol{v}'}{\partial t^2}\right|_{\boldsymbol{X}} - \bar{c}_s^2\,\underbrace{\nabla_{\boldsymbol{x}}\cdot(\nabla_{\boldsymbol{x}}\,\boldsymbol{v}')}_{\Delta_{\boldsymbol{x}}\boldsymbol{v}'} \approx \frac{1}{\bar{\rho}_0}\left(-\left.\frac{\partial}{\partial t}\right|_{\boldsymbol{X}}\left(\boldsymbol{Res}^{\boldsymbol{v}}(\overline{\boldsymbol{Y}};\bar{\boldsymbol{v}},\bar{p})\right)\right.
$$
$$
\left.(\gamma-1)\,\nabla_{\boldsymbol{x}}\left(Res^e(\overline{\boldsymbol{Y}};\bar{\boldsymbol{v}},\bar{p})\right)\right) \tag{2.65}
$$

$$
\left.\frac{\partial^2 p'}{\partial t^2}\right|_{\boldsymbol{X}} - \bar{c}_s^2\,\Delta_{\boldsymbol{x}}p' \approx \frac{c_s^2}{\bar{J}}\,\nabla_{\boldsymbol{x}}\cdot\boldsymbol{Res}^{\boldsymbol{v}}(\overline{\boldsymbol{Y}};\bar{\boldsymbol{v}},\bar{p})
$$
$$
-\frac{\gamma-1}{\bar{J}}\left.\frac{\partial}{\partial t}\right|_{\boldsymbol{X}}\left(Res^e(\overline{\boldsymbol{Y}};\bar{\boldsymbol{v}},\bar{p})\right) \tag{2.66}
$$

where $\Delta_{\boldsymbol{x}}$ is the Laplace operator in the Eulerian reference frame, and $\bar{c}_s = \sqrt{\frac{\gamma \bar{J}\bar{p}}{\bar{\rho}_0}}$ is the average speed of sound over the element.

Remark 14 *v_i' and p' can be considered as components of the error between the exact and numerically computed solution.*

Remark 15 *The operator $\mathcal{L}_{SH}$ represents the first-order vector form of a wave propagation differential operator, expressed by (2.65)–(2.66). This suggests that the errors in the solution for v and p are propagated in the form of acoustic waves excited by the (possibly distributional) derivatives of the residual $\boldsymbol{Res}(\boldsymbol{Y}^h)$.*

Remark 16 *Notice that $\boldsymbol{Res}^{\boldsymbol{v}}$ and Res^e contribute to each of the subgrid momentum and energy equations. The subgrid solution is therefore affected by a strong coupling in the residual contributions.*

Remark 17 *To complete the discussion, it is worthwhile to consider the subgrid equations for the displacements,*

$$\dot{\boldsymbol{u}}' = \boldsymbol{v}' - (\dot{\boldsymbol{u}}^h - \boldsymbol{v}^h), \qquad \text{in} \quad \mathcal{V}'(Q_n^e) \tag{2.67}$$

from which we learn that the rate of $\boldsymbol{u}'$ is driven by the residual in the mesh-scale displacement equations and the subgrid-scale velocity, $\boldsymbol{v}'$. $\boldsymbol{u}'$ is accumulated on each element and does not "transport" to neighbors: In this sense, its dynamics is tied to the entropy (or, material) wave, rather than the acoustic waves.

Chapter 3

A multiscale discourse on Galilean invariance

Although never required in standard Eulerian SUPG formulations, it was found of crucial importance in Lagrangian computations to ensure Galilean invariance of the SUPG operator. The aim of this discussion is to develop SUPG formulations whose stability properties are invariant with respect to a change of observer. For this purpose, it is paramount to develop a deep understanding of how a Galilean mapping affects the variational multiscale framework. In Eulerian coordintates, a Galilean transformation is given by

$$
\begin{bmatrix} \hat{t} \\ \hat{\boldsymbol{x}} \\ \hat{\boldsymbol{v}} \end{bmatrix} = \begin{bmatrix} 1 & \boldsymbol{0}_{1\times3} & \boldsymbol{0}_{1\times3} \\ -\boldsymbol{V}^G & \boldsymbol{I}_{3\times3} & \boldsymbol{0}_{3\times3} \\ \boldsymbol{0}_{3\times1} & \boldsymbol{0}_{3\times3} & \boldsymbol{I}_{3\times3} \end{bmatrix} \begin{bmatrix} t \\ \boldsymbol{x} \\ \boldsymbol{v} \end{bmatrix} - \begin{bmatrix} 0 \\ \boldsymbol{0} \\ \boldsymbol{V}^G \end{bmatrix} \tag{3.1}
$$

where $\hat{}$ stands for a tranformed vector or scalar quantity. Recalling that the Eulerian and Lagrangian coordinates coincide at $t = 0$, that is $\boldsymbol{x}(\boldsymbol{X}, 0) = \boldsymbol{X}$, it is easy to verify that, in the material reference frame,

$$
\begin{bmatrix} \hat{t} \\ \hat{\boldsymbol{X}} \\ \hat{\boldsymbol{v}} \end{bmatrix} = \begin{bmatrix} t \\ \boldsymbol{X} \\ \boldsymbol{v} - \boldsymbol{V}^G \end{bmatrix}, \quad \text{or,} \quad \begin{bmatrix} t \\ \boldsymbol{X} \\ \boldsymbol{v} \end{bmatrix} = \begin{bmatrix} \hat{t} \\ \hat{\boldsymbol{X}} \\ \hat{\boldsymbol{v}} + \boldsymbol{V}^G \end{bmatrix} \tag{3.2}
$$

Therefore, only the velocity transforms, while the time and material coordinates are invariant.

Applying a Galilean transformation to (2.36)–(2.37) yields

$$
Res_i^{\boldsymbol{v}}(\boldsymbol{Y}, \rho_0; p, \boldsymbol{v}) \quad \xrightarrow{G} \quad Res_i^{\boldsymbol{v}}(\hat{\boldsymbol{Y}}, \rho_0; p, \hat{\boldsymbol{v}}) \tag{3.3}
$$

$$
Res^E(\boldsymbol{Y}, \rho_0; p, \boldsymbol{v}) \quad \xrightarrow{G} \quad Res^E(\hat{\boldsymbol{Y}}, \rho_0; p, \hat{\boldsymbol{v}}) + V_i^G Res_i^{\boldsymbol{v}}(\hat{\boldsymbol{Y}}, \rho_0; p, \hat{\boldsymbol{v}}) \tag{3.4}
$$

As expected, the equations transform appropriately, and it is important to realize why: The scalar product of $\boldsymbol{Res^v}$ times $\boldsymbol{V}^G$ in the transformed total energy residual vanishes, since $\boldsymbol{Res^v}$ annihilates exactly.

Consider a Galerkin approximation of the Euler equations (without any stabilization) for which the residuals (2.36)–(2.37) are tested on the same function space used to represent the discrete solution. By the definition of Galerkin method, the *projection* of (2.36)–(2.37) onto the test function space must vanish. Therefore, the discrete Galerkin equations enjoy the same invariance properties of the exact equations, due to the fact that $\boldsymbol{V}^G$ is a constant and factors out of all integrals in the variational statement.

Remark 18 *Clearly, the discrete, non-vanishing, SUPG approximations to the residuals $\boldsymbol{Res^v}$ and Res^e in (2.38)–(??) are invariant, due to their "advective" structure. This observation is the foundation of the proposed "minimal" approach which guarantees invariant SUPG operators. Notice also that a discrete non-vanishing approximation to the total energy residual Res^E is not Galilean invariant, because of the presence of the kinetic energy term*

$$v_i Res_i^v(\boldsymbol{Y}, \rho_0; p, \boldsymbol{v}) \xrightarrow{G} \left(\hat{v}_i + V_i^G\right) Res_i^v(\hat{\boldsymbol{Y}}, \rho_0; p, \hat{\boldsymbol{v}}) \tag{3.5}$$

which is not invariant in the case $Res_i^v \neq 0$.

Let us now consider an SUPG method, that is, a Petrov-Galerkin finite element method, in which the perturbation of the Galerkin test function, $-\mathcal{L}_{SH}^* \boldsymbol{W}^h \cdot \boldsymbol{\tau}$, is obtained from a local linearization of the generalized advection operator. For the correctness of the stabilized method, it is essential to require that the perturbation to the test space be Galilean invariant, otherwise the stability properties of the SUPG stabilization operator may be *observer-dependent*, which is clearly unacceptable.

Remark 19 *A Galilean invariant form of $-\mathcal{L}_{SH}^* \boldsymbol{W}^h \cdot \boldsymbol{\tau}$ can be obtained using the matrices $\boldsymbol{A}_0$, $\boldsymbol{A}_i$, $\boldsymbol{C}$, as detailed in (2.16)–(2.17). These matrices take advantage of the "minimal" approach, since they are derived only from the momentum residual $\boldsymbol{Res^v}$ and internal energy residual Res^e.*

Clearly, all terms depending on thermodynamic variables and terms representing differences of kinematic or thermodynamic variables will be unaffected by a Galilean transformation. Therefore, the fine-scale vector $\boldsymbol{Y}'$ is an invariant. To prove this point, notice that the only term in $\boldsymbol{Y}'$ which needs additional analysis is the subgrid velocity $\boldsymbol{v}'$, since the displacement are expressed as difference of point locations, and the thermodynamic variables are invariant by definition.

$$\boldsymbol{v}' = \boldsymbol{v} - \boldsymbol{v}^h = \hat{\boldsymbol{v}} + \boldsymbol{V}^G - \hat{\boldsymbol{v}}^h - \boldsymbol{V}^G = \hat{\boldsymbol{v}}' \tag{3.6}$$

26

Remark 20 *An invariant approximation $\boldsymbol{Y}' \approx -\boldsymbol{\tau}\,\boldsymbol{Res}(\boldsymbol{Y}^h)$ is obtained by using the "minimal" residuals (2.46)–(2.47). The flux Jacobians $\boldsymbol{A}_0$, $\boldsymbol{A}_i$, and $\boldsymbol{C}$ used in the computation of the $\boldsymbol{\tau}$ stabilization matrix, have to be in the form (2.16)–(2.17).*

Combining the analysis of the invariance properties of the test function perturbation and the subgrid-scale solution (Remark 20), it is easily concluded that the SUPG operator must be invariant in its *entirety*.

3.1   The absence of a "multiscale paradox"

From the previous discussion it may seem that the variational multiscale framework is at stake. This is far from been the case, and to clear possible doubts, let us review more carefully the steps in which the multiscale analysis unfolds. The key equations are (2.24) and (2.29), presented below for convenience:

$$\mathcal{B}(\boldsymbol{W}^h, \boldsymbol{Y}^h) + \int_{Q_n} \mathcal{L}_{SH}^* \boldsymbol{W}^h \cdot \boldsymbol{Y}'\, dQ = 0 \qquad (3.7)$$

$$\boldsymbol{Y}' \;=\; \mathcal{L}_{SH}^{-1}(-\boldsymbol{Res}(\boldsymbol{Y}^h)) = -\int_{Q_n} \boldsymbol{G}_{SH}'\, \boldsymbol{Res}(\boldsymbol{Y}^h)\, dQ, \text{ in } \mathcal{V}'(Q_n) \qquad (3.8)$$

Let us assume now that $\mathcal{L}_{SH}^*$ in (3.7) and $\mathcal{L}_{SH}$ in (3.8) are obtained using the full Fréchet derivative of the Galerkin residual, rather than the minimal approach in [7]. It is clear that both equations have undergone a linearization, which causes second-order Galilean inconsistencies. It was observed in numerical computations discussed in section 3.2, that these inconsistencies had little or no effect on the quality of the results.

In theory, when the *exact* solution $\boldsymbol{Y}'$ to the linearized subgrid problem (3.8) is inserted into the mesh-scale equation (3.7), only second-order Galilean inconsistencies should be generated. In practice, the approximation $\boldsymbol{Y}' = -\boldsymbol{\tau}(\boldsymbol{X};t)\,\boldsymbol{Res}(\boldsymbol{Y}^h(\boldsymbol{X};t))$ is too coarse to retain all the required information on invariance, especially when used to generate the perturbation to the Galerkin test function in the SUPG operator.

The approach proposed in [7] is a way to remove Galilean inconsistencies from the approximation to the subgrid-scale dynamics provided by the SUPG operator.
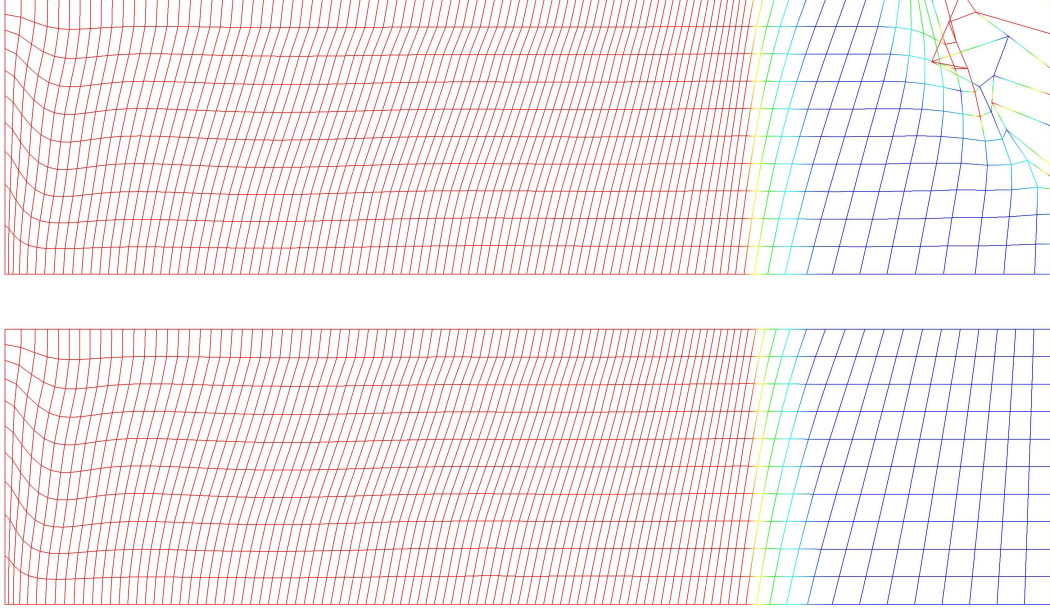
Figure 3.1. Pressure color plot on the mesh deformation outline. Above: SUPG formulation violating Galilean invariance. Below: SUPG abiding the Galilean invariance principle. A classical quadrilateral Saltzmann mesh is used in an implosion computation. The initial velocity is of unit magnitude and directed horizontally from right to left, except the left boundary which is held fixed. The initial density is unity and the initial specific internal energy is 10^{-1}. A shock forms at the left boundary and advances to the right. Note the *mesh coasting* phenomenon on the top right corner of the upper domain, absent in the SUPG formulation satisfying Galilean invariance, below.

3.2 Numerical investigations on Galilean invariance and stability

When a Saltzmann mesh is used in a planar implosion computation, lack of Galilean invariance leads to disastrous results. On the top right corner of the upper computational grid in Figure 3.1, the well known *coasting* phenomenon takes place, a manifestation of hourglass-type instabilities, accompanied by a large spurious peak in the pressure. In that portion of the domain, no shock is present, and a simple translational motion with unit velocity from right to left should occur. The correct behavior is instead captured by an SUPG formulation abiding the Galilean invariance principle, as shown in the bottom part of Figure 3.1.

Remark 21 *In a different test, the perturbation to the test function was computed using the Galilean invariant approach, but the residuals in the SUPG terms were evaluated in the non-invariant form. The computations were stable indicating that the invariance requirements on the test function perturbation, embedding the stability properties of the method, are far more stringent than the requirement on the residuals. This may also depend on the fact that the Galilean inconsistency on the residual is a higher-order term.*

3.3 Galilean invariance in the one-dimensional case

A more practical understanding of the key issues regarding Galilean invariance can be gained by analyzing the one-dimensional case for ideal gases. Let us apply the "standard" (non invariant) derivation proposed in [8] to the Lagrangian hydrodynamics formulation and evaluate the resulting stabilization operator. From the discussion in Remark 18, it is clear that the discrete residual would not be invariant. Let us then focus on the particular form assumed by the perturbation of the Bubnov-Galerkin test function provided by the SUPG stabilization. With manipulations analogous to [7], the flux Jacobians for the momentum and energy equations are readily obtained:

$$
\boldsymbol{A}_0 = \begin{bmatrix} \rho_0 & 0 \\ \rho_0 v & \frac{J}{\gamma-1} \end{bmatrix} \quad , \quad \boldsymbol{A}_1 = \begin{bmatrix} 0 & 1 \\ \frac{\gamma}{\gamma-1}p & v \end{bmatrix} \tag{3.9}
$$

The derivations of appendix A yield

$$
\boldsymbol{\tau} \;=\; \frac{\Delta t}{2\sqrt{1+\alpha^2}} \begin{bmatrix} \frac{1}{\rho_0} & 0 \\ -\frac{\gamma-1}{J}v & \frac{\gamma-1}{J} \end{bmatrix} \tag{3.10}
$$

where $\alpha = \frac{c_s \Delta t}{J \Delta X}$ is the Courant number. For the formulation in [7], the test function $\boldsymbol{W}^h$ is constant in time, so that $\partial_t \boldsymbol{W}^h = \boldsymbol{0}$. Also, $\boldsymbol{C}$ does not contribute to the energy or momentum equations, so that:

$$
\begin{aligned}
-\mathcal{L}_{SH}^* \boldsymbol{W}^h \cdot \boldsymbol{A}_i \boldsymbol{\tau} \;&=\; \partial_i \boldsymbol{W}^h \cdot \boldsymbol{A}_i \boldsymbol{\tau} \\
&=\; \partial_1 \boldsymbol{W}^h \cdot \boldsymbol{A}_1 \boldsymbol{\tau} \\
&=\; \partial_X \boldsymbol{W}^h \begin{bmatrix} 0 & 1 \\ \frac{\gamma}{\gamma-1}p & v \end{bmatrix} \frac{\Delta t}{2\sqrt{1+\alpha^2}} \begin{bmatrix} \frac{1}{\rho_0} & 0 \\ -\frac{\gamma-1}{J}v & \frac{\gamma-1}{J} \end{bmatrix} \\
&=\; \partial_X \boldsymbol{W}^h \frac{\Delta t}{2\sqrt{1+\alpha^2}} \begin{bmatrix} 0 & 1 \\ \frac{\gamma}{\gamma-1}p & v \end{bmatrix} \begin{bmatrix} \frac{1}{\rho_0} & 0 \\ -\frac{\gamma-1}{J}v & \frac{\gamma-1}{J} \end{bmatrix} \\
&=\; \partial_X \boldsymbol{W}^h \frac{\Delta t}{2\sqrt{1+\alpha^2}} \begin{bmatrix} -\frac{\gamma-1}{J}v & \frac{\gamma-1}{J} \\ \frac{\gamma}{\gamma-1}\frac{p}{\rho_0} - \frac{\gamma-1}{J}v^2 & \frac{\gamma-1}{J}v \end{bmatrix} \tag{3.11}
\end{aligned}
$$

Therefore, the "standard" SUPG perturbation to the Bubnov-Galerkin test function is *observer-dependent*, and more generally, a standard SUPG operator *is not* Galilean invariant. Let us consider the integrand $\mathcal{L}_{SH}^* \boldsymbol{W}^h \cdot \boldsymbol{\tau} \mathcal{L}_{SH} \boldsymbol{Y}^h$ in the stabilization term:

$$(-\boldsymbol{A}_0^T \partial_t - \boldsymbol{A}_j^T \partial_j) \boldsymbol{W}^h \cdot \boldsymbol{\tau} (\boldsymbol{A}_0 \partial_t + \boldsymbol{A}_i \partial_i) \boldsymbol{Y}^h$$

$$= -\partial_j \boldsymbol{W}^h \cdot \boldsymbol{A}_j \boldsymbol{\tau} \boldsymbol{A}_0 \; \partial_t \boldsymbol{Y}^h - \partial_j \boldsymbol{W}^h \cdot \boldsymbol{A}_j \boldsymbol{\tau} \boldsymbol{A}_i \; \partial_i \boldsymbol{Y}^h$$

$$= -\partial_X \boldsymbol{W}^h \cdot \boldsymbol{A}_1 \boldsymbol{\tau} \boldsymbol{A}_0 \; \partial_t \boldsymbol{Y}^h - \partial_X \boldsymbol{W}^h \cdot \boldsymbol{A}_1 \boldsymbol{\tau} \boldsymbol{A}_1 \; \partial_X \boldsymbol{Y}^h \tag{3.12}$$

where the contribution of $\boldsymbol{C}$ has been omitted, since it appears only in the displacement equation. The term $\partial_X \boldsymbol{W}^h \cdot \boldsymbol{A}_1 \boldsymbol{\tau} \boldsymbol{A}_1 \; \partial_X \boldsymbol{Y}^h$ represents the variational discretization of a diffusion operator, with an *artificial diffusion* matrix given by $\boldsymbol{A}_1 \boldsymbol{\tau} \boldsymbol{A}_1$. This term plays a key role in the stabilization of the Galerkin discretization, and represents the upwinding effect in the generalized streamline direction (the direction of propagation of acoustic waves, in the Lagrangian hydrodynamics case). It is easily realized that the SUPG numerical viscosity is also affected by the lack of Galilean invariance.

$$\boldsymbol{A}_1 \boldsymbol{\tau} \boldsymbol{A}_1 = \frac{\Delta t}{2\sqrt{1+\alpha^2}} \begin{bmatrix} -\frac{\gamma-1}{J}v & \frac{\gamma-1}{J} \\ \frac{\gamma}{\gamma-1}\frac{p}{\rho_0} - \frac{\gamma-1}{J}v^2 & \frac{\gamma-1}{J}v \end{bmatrix} \begin{bmatrix} 0 & 1 \\ \frac{\gamma}{\gamma-1}p & v \end{bmatrix}$$

$$= \frac{\Delta t}{2\sqrt{1+\alpha^2}} \begin{bmatrix} \frac{\gamma}{J}p & 0 \\ \frac{\gamma}{J}p v & \frac{\gamma}{\gamma-1}\frac{p}{\rho_0} \end{bmatrix} \tag{3.13}$$

The velocity v in the bottom left entry of the SUPG viscosity matrix could change both in magnitude and *sign*, if the computational domain undergoes a Galilean transformation, with potentially very dangerous consequences on the stabilization properties of the SUPG operator. A similar discussion applies in multiple dimensions.

Remark 22 *The instabilities detected for the tests presented in Figure 3.1 disappear for very low values of the pressure initial condition. In fact, the stabilizing viscosity matrix (3.13) vanishes as the pressure tends to zero, with a mitigating effect on its off-diagonal velocity entries. Only for moderate-to-high initial pressures, the effect of the off-diagonal terms containing the velocity is significant. It is interesting to notice that the intensity of the shock in a piston problem increases as the initial pressure decreases, if the initial density ρ_0 remains unchanged. Thus, weaker shock conditions actually yield the worst case scenario for the non-invariant SUPG stabilization.*

Chapter 4

Physical significance of stabilization and Kuropatenko analysis

Let us now analyze in more detail the physical significance of the stabilization operator. It was already mentioned in section 2.2.3 that the subgrid scale problem has an acoustic wave propagation nature. It will be now shown that there exists a very tight link between SUPG stabilization and the artificial viscosity concept developed by Kuropatenko [5] for weak shocks. To investigate the physical significance of the SUPG term, let us evaluate its viscosity matrix for the case of an ideal gas in one dimension.

4.1 A simple derivation for one-dimensional gas dynamics

Using the definition of $\boldsymbol{\tau}$ given in [7], the SUPG viscosity matrix reads

$$
\begin{aligned}
\boldsymbol{A}_1 \boldsymbol{\tau} \boldsymbol{A}_1 &= \begin{bmatrix} 0 & 1 \\ \frac{\gamma}{\gamma-1}p & 0 \end{bmatrix} \frac{\Delta t}{2\,CFL} \begin{bmatrix} \frac{1}{\rho_0} & 0 \\ 0 & \frac{\gamma-1}{J} \end{bmatrix} \begin{bmatrix} 0 & 1 \\ \frac{\gamma}{\gamma-1}p & 0 \end{bmatrix} \\
&= \frac{\Delta t}{2\,CFL} \begin{bmatrix} 0 & \frac{\gamma-1}{J} \\ \frac{\gamma\,p}{(\gamma-1)\,\rho_0} & 0 \end{bmatrix} \begin{bmatrix} 0 & 1 \\ \frac{\gamma}{\gamma-1}p & 0 \end{bmatrix} \\
&= \frac{\Delta t}{2\,CFL} \frac{\gamma\,J\,p}{\rho_0} \begin{bmatrix} \frac{\rho_0}{J^2} & 0 \\ 0 & \frac{1}{(\gamma-1)J} \end{bmatrix} \\
&= \frac{\Delta t}{2\,CFL} \frac{c_s^2}{J^2} \begin{bmatrix} \rho_0 & 0 \\ 0 & \frac{J}{\gamma-1} \end{bmatrix}
\end{aligned}
\tag{4.1}
$$

where $c_s = \sqrt{\frac{\gamma\, J\, p}{\rho_0}}$ is the speed of sound.

Remark 23 *Comparing with (3.13), it is noticeable the absence of any velocity term in the entries of (4.1).*

Let us further manipulate (4.1):

$$
\int_{Q_n^e(X)} \partial_i \boldsymbol{W}^h \cdot \boldsymbol{A}_1 \boldsymbol{\tau} \boldsymbol{A}_1 \partial_i \boldsymbol{Y}^h dQ_X
$$

$$
= \int_{Q_n^e(X)} \begin{bmatrix} \partial_X w_v^h \\ \partial_X w_p^h \end{bmatrix}^T \frac{\Delta t}{2\,CFL} \frac{c_s^2}{J^2} \begin{bmatrix} \rho_0 & 0 \\ 0 & \frac{J}{\gamma-1} \end{bmatrix} \begin{bmatrix} \partial_X v^h \\ \partial_X p^h \end{bmatrix} dQ_X
$$

$$
= \int_{Q_n^e(x)} \begin{bmatrix} \partial_x w_v^h \\ \partial_x w_p^h \end{bmatrix}^T \frac{\Delta t\, c_s^2}{2\,CFL} \begin{bmatrix} \frac{\rho_0}{J} & 0 \\ 0 & \frac{1}{\gamma-1} \end{bmatrix} \begin{bmatrix} \partial_x v^h \\ \partial_x p^h \end{bmatrix} dQ_x \tag{4.2}
$$

where the transformation from the reference to the current configuration has been performed, and the identities $\partial_x = J\,\partial_x$ and $dQ_x = J\,dQ_X$ have been used.

Considering the momentum contribution in (4.2), the stabilization is equivalent to a dissipative term with numerical viscosity

$$
\nu_{SUPG} \;=\; \frac{\rho_0}{J} \frac{\Delta t\, c_s^2}{2\,CFL} = \rho c_s \frac{\Delta t\, c_s}{2\,CFL} \tag{4.3}
$$

where the identity $\rho_0 = \rho J$ has been used. If the simulation runs close to $CFL = 1$, then $c_s \Delta t \approx \Delta x$, and

$$
\boxed{\nu_{SUPG} \approx \frac{\rho c_s \Delta x}{2}} \tag{4.4}
$$

Remark 24 *Expression (4.4) bears striking similarities with the Kuropatenko [5] viscosity in the limit for weak shocks, the only difference being the constant multiplier. In the general case, however, ν_{SUPG} scales like $c_s^2 \Delta t$.*

Remark 25 *The SUPG viscosity is active on the entire computational domain, while the Kuropatenko viscosity is active only in compression. At this point, questions about the accuracy of the overall SUPG formulation may arise for the reader unfamiliar with the SUPG stabilization concept, since it is well known that the Kuropatenko viscosity is only first-order accurate. It should not be forgotten, however, that the SUPG stabilization, being residual-based, is consistent, and the accuracy is not degraded to first order. An intuitive argument for this is that the $\boldsymbol{\tau}$ tensor is first order in the time increment and is multiplied by the residual, yielding a higher-order term.*

Remark 26 *Stabilization also acts on the energy equation.*

Chapter 5

Conclusions

The nature of the SUPG stabilization operator has been studied using the variational multiscale paradigm.

It is the hope of the author that this work could help in bridging the gap between the two communities investigating SUPG methods and algorithms for shock hydrodynamics computations. To this goal, it has been shown that the residual-based SUPG operator acts to prevent acoustical instabilities, and connections with the Kuropatenko viscosity correction in the limit of weak shocks have been highlighted.

The importance of Galilean invariance in the design of the stabilization operator has been discussed, shedding light on an overlooked aspect in standard SUPG approaches. Galilean invariance becomes very important also in applications different from compressible Lagrangian hydrodynamics, such as compressible turbulence. Given the current trend [1, 6] of developing turbulence models using the SUPG approximation to the subgrid-scale solution, it seems important to evaluate also in the case of turbulent compressible flow simulations whether or not Galilean invariance is satisfied and what its role is on the accuracy, robustness and reliability of simulations.

Appendix A

One-dimensional stabilization for ideal gases

In the following derivations, $\boldsymbol{A}_0$ and $\boldsymbol{A}_i$ refer only to the momentum and energy equations, since stabilization is not applied to the ODE relating rate of displacements to velocities. The multi-dimensional definition given by Shakib, Hughes and Johan [8], a fairly standard definition of the $\boldsymbol{\tau}$ matrix, reads:

$$\boldsymbol{\tau} = \boldsymbol{A}_0^{-1} \left(\boldsymbol{C}^2 + \left(\frac{\partial \xi_0}{\partial t} \right)^2 \boldsymbol{I} + \frac{\partial \xi_i}{\partial X_j} \frac{\partial \xi_i}{\partial X_k} \hat{\boldsymbol{A}}_j \hat{\boldsymbol{A}}_k \right)^{-1/2} \tag{A.1}$$

where $\hat{\boldsymbol{A}}_1 = \boldsymbol{A}_1 \boldsymbol{A}_0^{-1}$ and ξ_i are the coordinates in the parent domain of each element, and ξ_0 refers to the time axis. For an ideal gas in one dimension, and assuming the non-Galilean invariant approach to stabilization,

$$\frac{\partial \xi_i}{\partial X_j} \frac{\partial \xi_i}{\partial X_k} \hat{\boldsymbol{A}}_j \hat{\boldsymbol{A}}_k = \left(\frac{2}{\Delta X} \right)^2 \hat{\boldsymbol{A}}_1^{~2} \tag{A.2}$$

with

$$\boldsymbol{A}_0 = \begin{bmatrix} \rho_0 & 0 \\ \rho_0 v & \frac{J}{\gamma-1} \end{bmatrix}, \qquad \boldsymbol{A}_1 = \begin{bmatrix} 0 & 1 \\ \frac{\gamma}{\gamma-1}p & v \end{bmatrix} \tag{A.3}$$

Notice the presence of the velocity v in some of the entries of $\boldsymbol{A}_0$ and $\boldsymbol{A}_1$, due to the kinetic energy terms in the total energy equation. Then:

$$
\begin{aligned}
\hat{\boldsymbol{A}}_1 = \boldsymbol{A}_1 \boldsymbol{A}_0^{-1} &= \begin{bmatrix} 0 & 1 \\ \frac{\gamma}{\gamma-1}p & v \end{bmatrix} \begin{bmatrix} \rho_0 & 0 \\ \rho_0 v & \frac{J}{\gamma-1} \end{bmatrix}^{-1} = \begin{bmatrix} 0 & 1 \\ \frac{\gamma}{\gamma-1}p & v \end{bmatrix} \begin{bmatrix} \frac{1}{\rho_0} & 0 \\ -\frac{\gamma-1}{J}v & \frac{\gamma-1}{J} \end{bmatrix} \\
&= \begin{bmatrix} -\frac{\gamma-1}{J}v & \frac{\gamma-1}{J} \\ \frac{\gamma}{\gamma-1}\frac{p}{\rho_0} - \frac{\gamma-1}{J}v^2 & \frac{\gamma-1}{J}v \end{bmatrix} \tag{A.4}
\end{aligned}
$$

$$\hat{\boldsymbol{A}}_1^{~2} = \begin{bmatrix} \frac{\gamma p}{\rho_0 J} & 0 \\ 0 & \frac{\gamma p}{\rho_0 J} \end{bmatrix} = \left(\frac{c_s}{J} \right)^2 \boldsymbol{I}_{2\times2} \tag{A.5}$$

with $c_s = \sqrt{\frac{\gamma p}{\rho}} = \sqrt{\frac{\gamma p J}{\rho_0}}$. It is important to realize that the form of the SUPG stabilization is dependent on the function spaces adopted, and in particular on the time-integration strategy. For the second-order time integrator developed in [7], $\frac{\partial \xi_0}{\partial t} = \frac{2}{\Delta t}$ and

$$
\begin{aligned}
\boldsymbol{\tau} &= \hat{\boldsymbol{A}}_0^{-1} \left(\left(\frac{2}{\Delta t} \right)^2 \boldsymbol{I}_{2\times 2} + \left(\frac{2\,c_s}{J\,\Delta X} \right)^2 \boldsymbol{I}_{2\times 2} \right)^{-1/2} \\
&= \frac{\Delta t/2}{\sqrt{1+\alpha^2}} \hat{\boldsymbol{A}}_0^{-1} \\
&= \frac{\Delta t}{2\sqrt{1+\alpha^2}} \begin{bmatrix} \frac{1}{\rho_0} & 0 \\ -\frac{\gamma-1}{J}v & \frac{\gamma-1}{J} \end{bmatrix}
\end{aligned}
\tag{A.6}
$$

where $\alpha = \frac{c_s \Delta t}{J \Delta X}$.

References

[1] T. J. R. Hughes, V. M. Calo, and G. Scovazzi. Variational and multiscale methods in turbulence. In *Proceedings of the XXI International Congress of Theoretical and Applied Mechanics*. IUTAM, Kluwer, 2004.

[2] T. J. R. Hughes and M. Mallet. A new finite element formulation for computational fluid dynamics: III. The generalized streamline operator for multidimensional advective-diffusive systems. *Computer Methods in Applied Mechanics and Engineering*, **58**:305–328, 1986.

[3] T.J.R. Hughes. Multiscale phenomena: Green's functions, the Dirichlet-to-Neumann formulation, subgrid-scale models, bubbles and the origin of stabilized methods. *Computer Methods in Applied Mechanics and Engineering*, **127**:387–401, 1995.

[4] T.J.R. Hughes, G.R. Feijóo, L. Mazzei, and J.-B. Quincy. The Variational Multiscale Method — a paradigm for computational mechanics. *Computer Methods in Applied Mechanics and Engineering*, **166**:3–24, 1998.

[5] V. F. Kuropatenko. On difference methods for the equations of hydrodynamics. In N. N. Janenko, editor, *Difference methods for solutions of problems of mathematical physics, I*. American Mathematical Society, Providence, RI, 1967.

[6] G. Scovazzi. *Multiscale methods in science and engineering*. PhD thesis, Mechanical Engineering Department, Stanford Universty, September 2004. Available at `http://www.cs.sandia.gov/~gscovaz/pubs.html`.

[7] G. Scovazzi, M. A. Christon, T. J. R. Hughes, and J. N. Shadid. Stabilized shock hydrodynamics: I. A Lagrangian method. *Computer Methods in Applied Mechanics and Engineering*, 2005. Submitted.

[8] F. Shakib, T. J. R. Hughes, and Z. Johan. A new finite element formulation for computational fluid dynamics: X. The compressible Euler and Navier-Stokes equations. *Computer Methods in Applied Mechanics and Engineering*, **89**:141–219, 1991.

[9] T. E. Tezduyar. Computation of moving boundaries and interfaces and stabilization parameters. *International Journal of Numerical Methods in Fluids*, **43**:555–575, 2003.

[10] T. E. Tezduyar. Determination of the stabilization and shock-capturing parameters in SUPG formulation of compressible flows. In *Proceedings of European Congress on Computational Methods in Applied Sciences and Engineering EC-COMAS 2004*, Jyäskylä, Finland, July 24-28, 2004.

[11] T. E. Tezduyar and M. Senga. Determination of the stabilization and shock-capturing parameters in SUPG formulation of compressible flows. In *Proceedings of WCCM VI in conjunction with APCOM04*, Beijing, China, September 5-10, 2004. Tsinghua University Press & Springer-Verlag.

[12] J. Von Neumann and R.D. Richtmyer. A method for the numerical computation of hydrodynamic shocks. *Journal of Applied Physics*, **21**:232–237, 1950.